

Gap solitons in optical lattices embedded into nonlocal media

YuanYao Lin¹, Chandroth P. Jisha¹, Ching-Jen Jeng¹, Ray-Kuang Lee¹, and Boris A. Malomed²

¹*Institute of Photonics Technologies, National Tsing-Hua University, Hsinchu 300, Taiwan*

²*Department of Physical Electronics, School of Electrical Engineering,
Faculty of Engineering, Tel Aviv University, Tel Aviv 69978, Israel.*

We analyze the existence, stability, and mobility of gap solitons (GSs) in a periodic photonic structure built into a nonlocal self-defocusing medium. Counter-intuitively, the GSs are supported even by a highly nonlocal nonlinearity, which makes the system quasi-linear. Unlike local models, the variational approximation (VA) predicts the GSs in a good agreement with numerical findings, due to the suppression of undulating tails of the solitons.

PACS numbers: 42.65.Tg, 42.65.Sf, 42.70.Qs

I. INTRODUCTION

Solitons are self-guided wave packets propagating in nonlinear media, maintaining the self-trapped shape. In particular, optical solitons are supported by the balance between the material nonlinearity and diffraction in the spatial domain or dispersion in the temporal domain [1]. As concerns spatial solitons in planar waveguides, it is well known that the self-focusing Kerr nonlinearity supports bright ones, while a defocusing nonlinearity admits dark solitons. Even in the absence of integrability, solitons readily feature quasi-particle collisions, with the outcome depending on the relative phase between them. These properties suggest to use solitons in various applications to all-optical data-processing schemes and telecommunication systems [2].

Efficient control of the transmission and localization of light may be provided by photonic crystals (PhCs), built as structures with periodic modulation of the refractive index (RI). They open the ways to tailor the dispersion, diffraction, and routing of electromagnetic waves [3]. Nonlinear PhCs, composed of appropriate materials, have revealed a wealth of nonlinear optical phenomena, including the self-trapping of localized modes in the form of the gap solitons (GSs) [4–6]. These modes can be formed in self-focusing and defocusing media alike, due to the possibility of the change in the sign of the effective dispersion/diffraction in PhCs. [7]. Experimentally, GSs were first created in the temporal domain, as solitons in a short piece of a fiber Bragg grating [8]. Technologies based on the use of reconfigurable (photoinduced) lattices, that have been implemented in photorefractive crystals [9] and nematic liquid crystals [10], offer new ways to control GSs in the spatial domain, by varying the lattice depth and spacings.

Combining the benefits of PhCs and solitons, GSs have considerable potential for the use in photonics. GSs of matter waves have also been theoretically studied [11] and experimentally created [12] in Bose-Einstein condensates formed by atoms with repulsive interactions, trapped in optical-lattice potentials. Bifurcations and stability of optical GSs were analyzed in PhCs with the local Kerr nonlinearity [13]. However, the limited mobility of GSs in the transverse directions, due to their pinning to the underlying lattice potentials [14], is an obstacle to the use of GSs in switching and routing operations [15, 16].

Recently, it has been predicted that solitons supported by a *nonlocal* nonlinearity, self-focusing or defocusing, in the combination with the effective diffraction induced by either the total internal reflection (ordinary solitons) [17] or bandgap spectrum [18], may move much easier across the lattice. Nonlocal effects come to play an important role as the characteristic correlation radius of the medium's response function becomes comparable to the transverse width of the wave packet [19]. Experimental observations of nonlocal responses have been demonstrated in various media, including photorefractive crystals [20], nematic liquid crystals [21], and thermo-optical materials [22, 23]. The nonlocal nonlinearity induces new features in the wave dynamics, modifying the underlying modulational [24], azimuthal [25], and transverse [26] instabilities. Suppression of the collapse of multidimensional solitons [27], a change of interactions between them [28], the formation of soliton bound states [29], merger of colliding solitons into a standing wave [30], and families of dark-bright soliton pairs [31] were also predicted recently.

The nonlocality is known to improve the stability of solitons due to the diffusion mechanism of the underlying nonlinearity. In the limit of strongly nonlocal nonlinearity, the system become an effectively linear one [32]. In such an extreme limit, the existence of GSs (for the defocusing sign of the nonlinearity) is questionable. In this work, we identify families of bright on-site and off-site GSs in self-defocusing nonlinear media by means of numerical methods and analytical methods. With the infinite range of the nonlocality, we demonstrate the existence of spatial GSs with a finite beam's width. The analytical consideration is based on the variational approximation (VA) with a Gaussian ansatz, similar to how it was applied to the matter-wave GSs in Refs. [33, 34]. Unlike the case of the local defocusing nonlinearity, in the nonlocal modes the Gaussian ansatz works well not only deep inside of the bandgap, but also close to its edge. The stability and mobility of the GS families in the nonlocal medium are investigated too.

II. THE MODEL AND NUMERICAL RESULTS FOR GAP SOLITONS

We consider a wave packet propagating along axis z in a PhC structure embedded into with a medium with the self-defocusing cubic nonlocal nonlinearity. A model widely adopted for the description of such media is [24, 35]

$$i\frac{\partial\Psi}{\partial z} = -\frac{1}{2}\frac{\partial^2}{\partial x^2}\Psi + V(x)\Psi + n\Psi, \quad (1)$$

$$n - d\frac{\partial^2}{\partial x^2}n = |\Psi|^2, \quad (2)$$

where Ψ is the amplitude of the electromagnetic wave, x the transverse coordinate, $n(x, z)$ a perturbation of the local RI corresponding to the intensity-response function with an exponential kernel, and d is a parameter which determines the degree of the nonlocality of the response. All the physical quantities and spacial coordinates are made

dimensionless by normalization procedure with respect to the input beam width, wavelength, and Kerr coefficient of the nonlinear material [1]. The limit of $d \rightarrow \infty$ corresponds to the well-known Zakharov's system, which is a fundamental model in plasma physics (for Langmuir waves) and other fields [36]. The PhC structure is represented by the periodic transverse potential, $V(x) = V_0 \sin^2 x$ (x is normalized so as to make the period equal to π). Stationary solutions with propagation constant μ are sought for as $\Psi(x, z) = \exp(-i\mu z)\phi(x)$, which gives rise to the stationary version of Eqs. (1) and (2):

$$\mu\phi = -\frac{1}{2}\phi_{xx} + V_0 \sin^2(x)\phi + n\phi, \quad (3)$$

$$n - d\frac{\partial^2 n}{\partial x^2} = |\phi|^2. \quad (4)$$

If the nonlinearity is omitted, Eq. (3) decouples from $n(x)$ and becomes a linear equation, which supports Bloch-wave solutions, $\phi(x) = f(x) \exp(i k x)$, where k is the quasi-wavenumber, and $f(x)$ is a periodic function with period π . As an example, we take $V_0 = 4$ and display the corresponding dispersion relation, including the three lowest three bands, in Fig. 1. From this diagram, it is seen that finite bandgaps are introduced by the periodic potential; in particular, the first finite bandgap covers a broad interval, $1.305 < \mu < 3.19$.

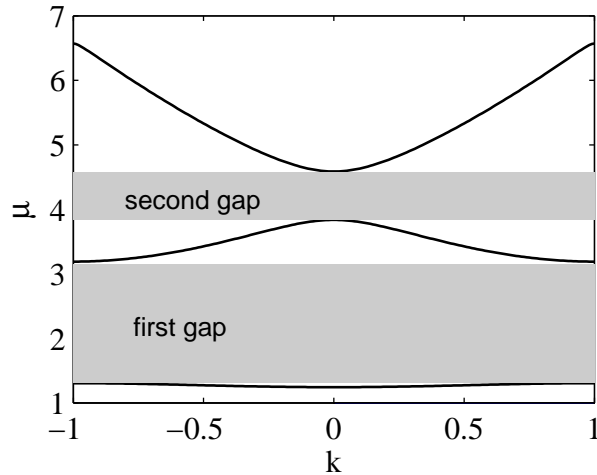


FIG. 1. A typical example of the spectrum, with quasi-wavenumber k , induced by the linearize version of Eq. (3), with $V_0 = 4$. Shaded areas are covered by the bandgaps.

The nonlinearity may give rise to x -periodic modes [37] or localized GSs [38], with μ falling into the bandgaps, which refers to *gap solitons*. Starting with the GS solution in the middle of the gap, we have found different families of bright solitons numerically, using by standard relaxation technique with boundary conditions $\phi(\pm\infty) = 0$. In Fig. 2, we demonstrate generic examples of the GS modes found in the first finite bandgap. Local (with $d = 0$), and nonlocal (for $d = 40$) on-site-centered GSs are shown near the bottom of the gap in Figs. 2(a, d), in the middle of the gap in Figs. 2(b, e), and close to the top edge in Figs. 2(c, f), with propagation constants $\mu = 1.31$, $\mu = 2.5$, and $\mu = 3.1$, respectively. Simplest higher-order GS solutions of the nonlocal model (off-site-centered solitons) are presented in Fig. 2(g-i). The two distinct types of the solitons, on-site and off-site, are defined by the position of their centers with respect to the underlying periodic potential [17, 39].

Similar to solitons in nonlocal media with the self-focusing nonlinearity [24, 35], the amplitude of the GSs in the present model increases at a higher degree of the nonlocality, d . As a result, the related total power, $\mathbf{P} \equiv \int_{-\infty}^{\infty} |\Psi(x)|^2 dx$, is a growing function of d , as shown in Fig. 3. In comparison to the local nonlinear medium, with $d = 0$ [see Figs. 2(a-c)], the width of the RI perturbation, w_n , becomes broader with the increase of d , for the focusing [24, 35] and defocusing signs of nonlinearity alike, due to the diffusion type of the nonlocal response. Relations between w_n and d are shown in the first column of Fig. 4. On the contrary to the solitons in self-focusing nonlocal media [17, 18], the beam's width of the GSs in the present case, w_b , decreases with the increase of d , as shown in the second column of Fig. 4. At very large values of d , the beam's width in the GS approaches a constant value.

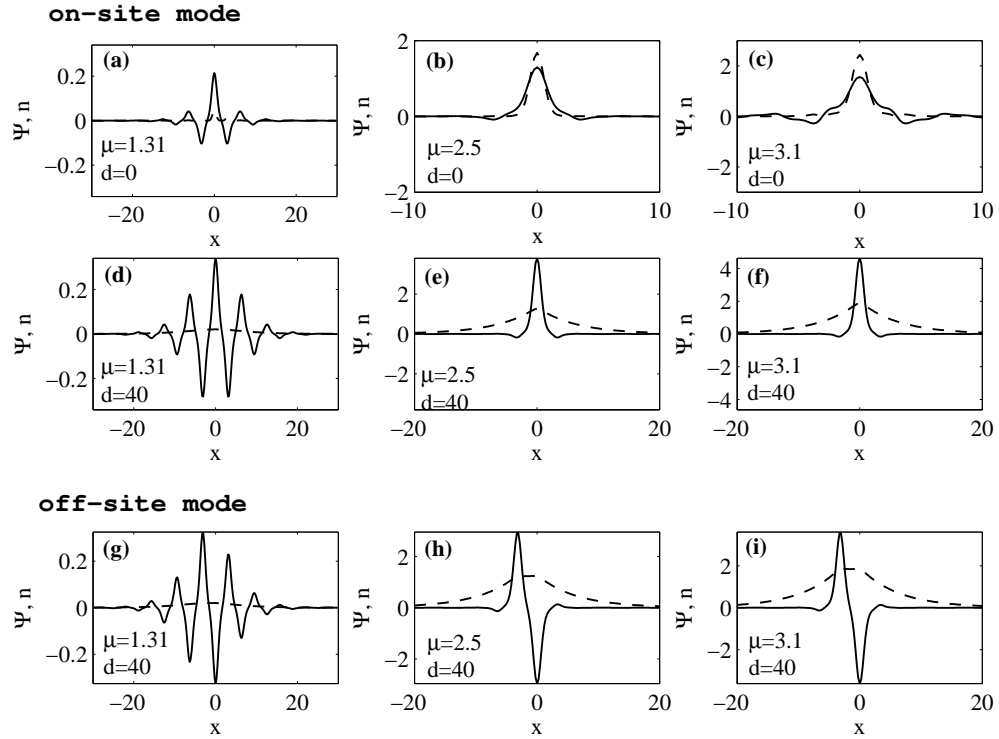


FIG. 2. Typical examples of gap-soliton modes in the first finite bandgap. (a-c): On-site solutions in the local model ($d = 0$). (b-f): On-site solutions for $d = 40$. (h-i): Off-site solution for $d = 40$. Solid lines show the field profiles, while the corresponding profiles of the refractive-index perturbation, $n(x)$, are plotted by dashed lines.

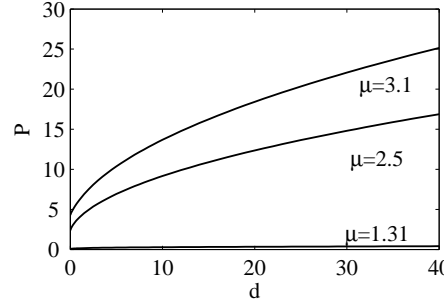


FIG. 3. The total power of on-site gap solitons versus the nonlocality parameter, d , for three distinct values of the propagation constant taken, respectively, near the bottom edge of the first finite bandgap's edge ($\mu = 1.31$), in the middle of the gap ($\mu = 2.5$), and approaching the top band edge ($\mu = 3.1$).

III. VARIATIONAL APPROXIMATION

It is well known that undulating tails in the shape of GSs, induced by the underlying periodic potential, make the Gaussian ansatz inappropriate as an approximation for GSs, especially close to bandgap edges [33]. However, Fig. 2 demonstrates that the nonlocal nonlinearity makes GSs in the present model more localized, suggesting to apply the VA. The Lagrangian density for Eq. (1) is

$$L = \frac{i}{2} (\phi_z^* \phi - \phi_z \phi^*) + k|\phi|^2 + \frac{1}{2} (\phi_x)^2 + V_0 \sin^2(x) |\phi|^2 + n|\phi|^2 - \frac{d}{2} (n_x)^2 - \frac{n^2}{2}, \quad (5)$$

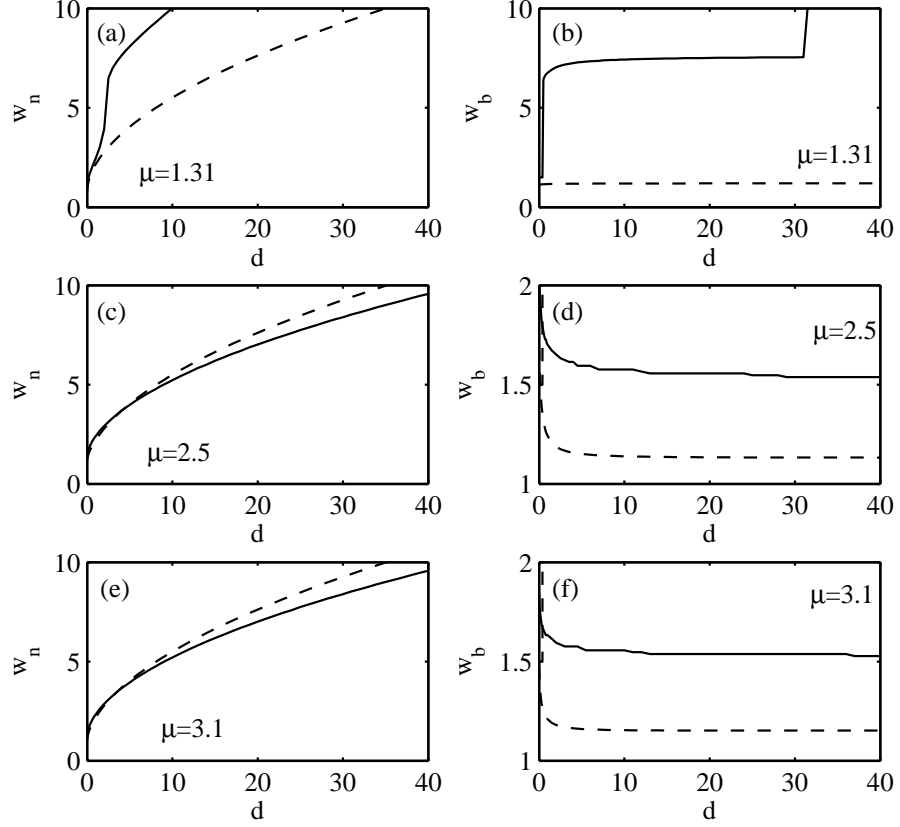


FIG. 4. Left column (a,c,e): The width of the refractive-index profile, w_n , in gap solitons, versus nonlocality parameter d . Right column (b,d,f): The width of the field component of the gap solitons, w_b , versus d . Numerical and variational results are shown by solid and dashed lines, respectively. The value of the propagation constant is fixed in each panel, as indicated.

Following the above argument, we adopt the Gaussian ansatz for field ϕ and RI perturbation n ,

$$\phi(x, z) = A(z) \exp \left[-\frac{x^2}{2w_b^2(z)} + ib(z)x^2 \right], \quad n(x, z) = C(z) \exp \left[-\frac{x^2}{2w_n^2(z)} \right], \quad (6)$$

with $A(z)$, $b(z)$ and $w_b(z)$ standing for the amplitude, chirp and width of the field component of the GS, while $C(z)$ and $w_n(z)$ are the amplitude and width of its RI counterpart. Substituting the ansatz into Lagrangian density (5) and performing the standard calculations [41], we arrive at VA-generated relations between the parameters,

$$\frac{1}{2w_b^2} = \frac{(3d + 2w_n^2)^2}{8w_n^4(2w_n^2 - d)^2} + \frac{\mathbf{P}(3d + 2w_n^2)}{2w_n(d + 2w_n^2)^3} - \frac{2w_n(3d + 2w_n^2)}{(d + 2w_n^2)^2} - (\mu + V_0), \quad (7)$$

$$w_b^2 = \frac{2w_n^2(2w_n^2 - d)}{3d + 2w_n^2}. \quad (8)$$

Using Eqs. (7) and (8), in Fig. 5 we draw the surface plot for the width of the RI profile, w_n , as a function of total power \mathbf{P} and nonlocality parameter d , at a fixed value of μ , and compare it to the numerical results. As expected, the VA produces good results for the GSs taken in the middle of bandgap – for instance, at $\mu = 2.5$.

In addition, using the power and propagation constant found numerically in Sec. II, we show in Fig. 4 that both numerical and variation solutions represent the same trend for the widths of both components of the GSs. In particular, for $\mu = 2.5$ and $\mu = 3.1$, as shown in Fig. 4(c-f), w_n increases as the square root of the nonlocality strength, d , in agreement with Ref. [32]. On the contrary, w_b drops to a finite value as d increases. However, for $\mu = 1.31$, which is very close to the edge of the first finite bandgap, the trend is completely different. This difference is explained by the known fact that GSs with the propagation constant taken very close to edges of bandgaps are similar to the linear Bloch waves in the linear lattice, as seen in Fig. 2(d). When the amplitude of the respective undulating tails in the GS shape is comparable to its main peak, the Gaussian ansatz definitely fails. Nevertheless, close to the top

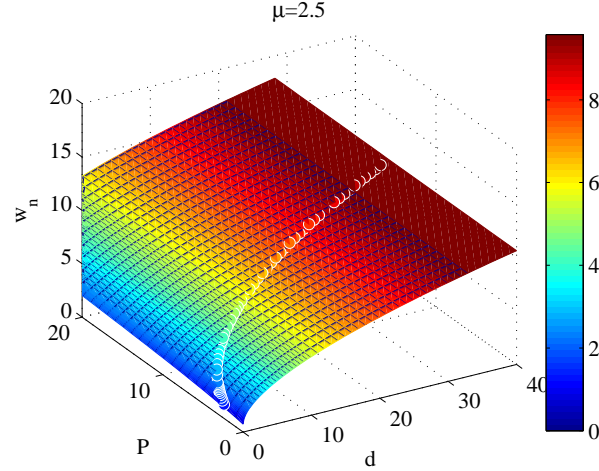


FIG. 5. (Color online) The surface plot for the width of the refractive- index component of the gap soliton, w_n , at $\mu = 2.5$, as predicted by variational equations (7), (8). The chain of dots represents full numerical solutions.

edge of the first finite bandgap – for instance, at $\mu = 3.1$, the ansatz still works well because the major peak in the GS profile remains much higher than the undulating tails in the entire nonlocality regime. Thus, the applicability condition for the Gaussian-based VA in the system with the self-defocusing nonlocal nonlinearity is clear: It is usable as long as the GS propagation constant is taken not too close to the bottom edge of the first finite bandgap.

In the extremely nonlocal regime, the field component in the GSs is much narrower than the RI profile. In this case, the RI profile may be approximated as $n(x) \approx R(x) \equiv e^{-|x|/\sqrt{d}}/(2\sqrt{d})$, where $R(x)$ is the RI response function. The corresponding width of the RI profile is $w_n \approx 2\sqrt{d} \ln 2$. Then, using the quasi-linear limit similar to that developed in Ref. [32], one can predict the threshold power necessary for the formation of the GS,

$$P_{\text{thr}} = 2(\mu - \mu_0)\sqrt{d}, \quad (9)$$

where μ_0 as the propagation constant at the edge of the first finite bandgap. The comparison to the numerical results in this extremely nonlocal regime is shown in Fig. 6.

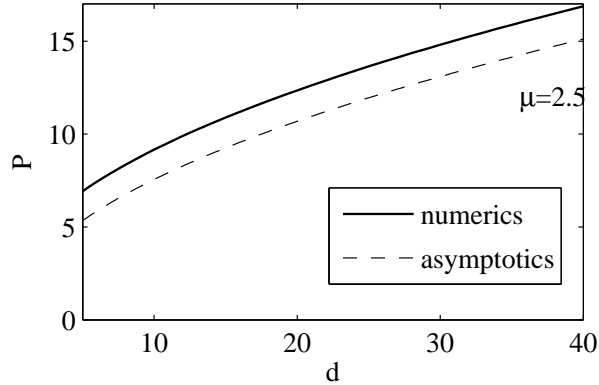


FIG. 6. The threshold power necessary for the formation of the gap solitons versus the nonlocality parameter, d . The solid and dashed lines depict, respectively, the numerical results and asymptotic approximation (9).

IV. STABILITY AND MOBILITY OF THE GAP SOLITONS

Having constructed the family of the GS solutions, we analyze their stability in the usual way, considering perturbed GS solutions as

$$u = u_0(x)e^{ibz} + \epsilon[p(x)e^{i\delta z} + q(x)e^{-i\delta^* z}]e^{ibz}, \quad (10)$$

$$n = n_0 + \Delta n, \quad (11)$$

where $\epsilon \ll 1$ is the perturbation amplitude, $u_0(x)$ is the unperturbed solution, and $\text{Im}\{\delta\}$ is the growth rate of the perturbations. Although the strengthening nonlocality makes the GS shape sharper and stronger localized, we have found, somewhat counter-intuitively, that the on-site GS family is still stable, while its off-site counterpart is not, cf. [13]. Figure 7(a) demonstrates that the nonlocality significantly reduces the growth rate of the unstable perturbation mode for off-site solitons, as in the case in the self-focusing nonlinearity [18]. Due to its diffusion character, the nonlocality smoothes down the undulating tails in the RI profile, $n(x)$. It is this smoothness that stabilizes GSs, for either sign of the nonlinearity. Therefore, as the strength of the nonlocality increases, the GS solutions become more stable, through the broadening of the effective potential.

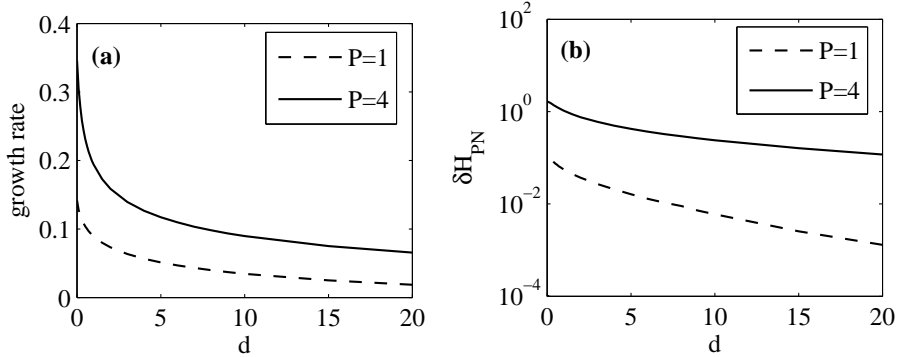


FIG. 7. (a) The instability growth rate and (b) the PN energy barrier versus the nonlocality strength, d , for different values of the total power, \mathbf{P} .

The mobility of the GSs in the present model was studied through calculating the respective Peierls-Nabarro (PN) potential barrier, which is defined as the height of an effective periodic potential generated by the underlying lattice. The potential barrier determines the minimum energy needed to move the center of mass of a localized wave packet by one lattice site [40]. As usual, we can calculate the PN barrier as the difference of values of the model's Hamiltonian (H) between on-site and off-site modes [17], i.e.,

$$\delta H = H_{\text{even}} - H_{\text{odd}}, \quad (12)$$

$$H \equiv \int_{-\infty}^{\infty} \left[-\frac{1}{2} \left| \frac{\partial u}{\partial x} \right|^2 - \frac{1}{2} |u|^2 n - V_x |u|^2 \right] dx. \quad (13)$$

As seen in Fig. 7(b), in the first finite bandgap the PN barrier is reduced in comparison to the case of the local nonlinearity, $d = 0$, which is a natural manifestation of the nonlocality.

V. CONCLUSION

We have reported the analysis of the existence, stability, and mobility of one-dimensional GSs (gap solitons) in the periodic potential structure combined with the self-defocusing nonlocal nonlinearity. We have found that the GSs become tighter localized in space, with a higher formation-power threshold. The results have been obtained in the numerical form and reproduced, with a reasonable accuracy, by the VA (variational approach). Using the linear-stability analysis and calculating the PN (Peierls-Nabarro) potential barrier, we have demonstrated that the GSs become not only more stable, but also more mobile, with the increase of the nonlocality. The comparison with the limit of the extreme nonlocality was reported too. Taking into regard the possibilities offered by the currently

available technology for fabricating nonlocal nonlinear media with controllable properties, such as photorefractive crystals, nematic liquid crystals and thermo-optical materials, the results reported in this work may suggest new possibilities for the design of soliton-based photonic devices. For instance, in photorefractive materials like SBN or LiNbO₃, photorefractive gratings [1] and self-defocusing nonlinearity [42] can be easily achieved by external electrical field properly applied across the crystal axis. Also in liquid-filled photonic crystal fibers [43], 2D band gap effect with thermal-type self-defocusing nonlinearity is demonstrated. It may also be interesting to extend the model and the analysis of GSs in it (including vortex solitons) to the two-dimensional geometry.

ACKNOWLEDGEMENT

This work is partly supported by the National Science Council of Taiwan with contrasts NSC 95-2112-M-007-058-MY3, NSC 95-2120-M-001-006 and NSC 98-2112-M-007-012.

[1] Yu. S. Kivshar and G. P. Agrawal, *Optical Solitons: from Fibers to Photonic Crystals*, (Academic, San Diego, California, 2003), and references therein.

[2] *Soliton-driven photonics*, edited by A. D. Boardman and A. P. Sukhorukov (Kluwer Academic Publishers, 2001).

[3] J. D. Joannopoulos, R. D. Meade, and J. N. Winn, *Photonic Crystals: Molding the Flow of Light*, (Princeton University Press, Princeton, 1995).

[4] C. M. de Sterke and J. E. Sipe, in *Progress in Optics*, Vol. XXXIII, p. 203, edited by E. Wolf (North-Holland, Amsterdam, 1994).

[5] S. F. Mingaleev and Yu. S. Kivshar, *Phys. Rev. Lett.* **86**, 5474 (2001).

[6] *Nonlinear Photonic Crystals*, edited by R. Slusher and B. Eggleton (Springer-Verlag, Berlin, 2003).

[7] E. A. Ostrovskaya and Yu. S. Kivshar, *Phys. Rev. Lett.* **90**, 160407 (2003).

[8] B. J. Eggleton, R. E. Slusher, C. M. de Sterke, P. A. Krug, and J. E. Sipe, *Phys. Rev. Lett.* **76**, 1627 (1996).

[9] N.K. Efremidis, S. Sears, D.N. Christodoulides, J.W. Fleischer, M. Segev, *Phys. Rev. E* **66**, 046602 (2002).

[10] M. Peccianti, K. A. Brzdkiewicz, and G. Assanto, *Opt. Lett.* **27**, 1460 (2002).

[11] V. A. Brazhnyi and V. V. Konotop, *Mod. Phys. Lett. B* **18**, 627 (2004).

[12] B. Eiermann, Th. Anker, M. Albiz, M. Taglieber, P. Treutlein, K.-P. Marzlin, and M. K. Oberthaler, *Phys. Rev. Lett.* **92**, 230401 (2004).

[13] D. E. Pelinovsky, A. A. Sukhorukov, and Yu. S. Kivshar, *Phys. Rev. E* **70**, 036618 (2004).

[14] H. Sakaguchi and B. A. Malomed, *J. Phys. B* **37**, 1443 (2004); **37**, 2225 (2004).

[15] D. N. Christodoulides, F. Lederer, and Y. Silberberg, *Nature (London)* **424**, 817 (2003).

[16] Y.V. Kartashov, V.A. Vysloukh, L. Torner, *Phys. Rev. Lett.* **93**, 153903 (2004).

[17] Z. Xu, Y. V. Kartashov, and L. Torner, *Phys. Rev. Lett.* **95**, 113901 (2005).

[18] Y. Y. Lin, I.-H. Chen, and R.-K. Lee, *J. Opt. A: Pure Appl. Opt.* **10**, 044017 (2008).

[19] W. Królikowski and O. Bang, *Phys. Rev. E* **63**, 016610 (2000).

[20] G. C. Duree *et al.*, *Phys. Rev. Lett.* **71**, 533-536 (1993).

[21] C. Conti, M. Peccianti, and G. Assanto, *Phys. Rev. Lett.* **91**, 073901 (2003).

[22] C. Rotschild, O. Cohen, O. Manela, M. Segev, and T. Carmon, *Phys. Rev. Lett.* **95**, 213904 (2005).

[23] N. K. Efremidis, *Phys. Rev. A* **77**, 063824 (2008).

[24] W. Królikowski, O. Bang, N. I. Nikolov, D. Neshev, J. Wyller, J. J. Rasmussen, and D. Edmundson, *J. Opt. B: Quant. Semiclassical Opt.* **6**, S288-S294 (2004).

[25] S. Lopez-Aguayo, A. S. Desyatnikov, and Yu. S. Kivshar, *Opt. Express* **14**, 7903-7908 (2006).

[26] Y. Y. Lin, R.-K. Lee, and Yu. S. Kivshar, *J. Opt. Soc. Am. B* **25**, 576 (2008).

[27] O. Bang, W. Królikowski, J. Wyller, and J. J. Rasmussen, *Phys. Rev. E* **66**, 046619 (2002).

[28] M. Peccianti, K. A. Brzdkiewicz, and G. Assanto, *Opt. Lett.* **27**, 1460-1462 (2002).

[29] Z. Xu, Y. V. Kartashov, and L. Torner, *Opt. Lett.* **30**, 3171-3173 (2005).

[30] Y. Y. Lin, R.-K. Lee, and B.A. Malomed, *Phys. Rev. A* **80**, 013838 (2009).

[31] Y. Y. Lin and R.-K. Lee, *Opt. Express* **15**, 8781 (2007).

[32] A. W. Snyder and D. J. Mitchell, *Science* **276**, 1538-1541 (1997).

[33] A. Gubeskys, B.A. Malomed, and I. M. Merhasin, *Stud. Appl. Math.* **115**, 255 (2005).

[34] S. Adhikari and B.A. Malomed, *Europhys. Lett.* **79**, 50003 (2007).

[35] W. Królikowski, O. Bang, J. J. Rasmussen, and J. Wyller, *Phys. Rev. E* **64**, 016612 (2001).

[36] V. E. Zakharov, *Zh. Eksp. Teor. Fiz.* **62**, 1745 (1972) [*Sov. Phys. JETP* **35**, 908 (1972)]; E. I. Shulman, *Dokl. Akad. Nauk SSSR* **259**, 578 (1981); L. Stenflo, *Phys. Scr.* **33**, 156 (1986).

[37] Y. Y Lin, R.-K. Lee, Y.-M. Kao, and T.-F. Jiang, *Phys. Rev. A* **78**, 023629 (2008).

[38] Y. Zhang, and B. Wu, *Phys. Rev. Lett.* **102**, 093905 (2009).

[39] B. J. Dabrowska, E. A. Ostrovskaya, and Yu. S. Kivshar, *J. Opt. B Quantum Semicl. Opt.* **6**, 423 (2004).

- [40] Yu. S. Kivshar and D. K. Campbell, *Phys. Rev. E* **48**, 3077-3081 (1993).
- [41] B. A. Malomed, in *Progress in Optics*, Vol. 43, p. 71, edited by E. Wolf (North-Holland, Amsterdam, 2002).
- [42] N. Zhu, R. Guo, S. Liu, Z. Liu and T. Song, "Spatial modulation instability in self-defocusing photorefractive crystal LiNbO₃:Fe," *J. Opt. A: Pure Appl. Opt.* **8**, 149-154 (2006).
- [43] C.R. Rosberg, F.H. Bennet, D.N. Neshev, P.D. Rasmussen, O. Bang, W. Krolikowski, A. Bjarklev, and Y.S. Kivshar, "Tunable diffraction and self-defocusing in liquid-filled photonic crystal fibers," *Opt. Express* **19**, 12145-12150 (2007).